Biochimica et Biophysica Acta, 1106 (1992) 273–281

BBAMEM 75618

Molecular packing parameters of bipolar lipids

F. Cavagnetto [a], A. Relini [a], Z. Mirghani [a], A. Gliozzi [a], D. Bertoia [b] and A. Gambacorta [c]

[a] *Dipartimento di Fisica, Università di Genova, Genova (Italy),* [b] *Istituto di Chimica Organica, Università di Genova, Genova (Italy) and* [c] *Istituto per la Chimica di Molecole di Interesse Biologico, Arco Felice, Napoli (Italy)*

(Received 30 December 1991)

Key words: Bipolar lipid; Self assembly; Monopolar-bipolar lipid vesicle; Ionic transport; Molecular packing parameter

The bipolar lipid fractions extracted from the thermophilic archaeobacterium *Sulfolobus solfataricus* have different chemical structures and geometrical shapes. The conditions which lead to the formation of vesicles were investigated in order to study the self-assembly of these molecules. Such conditions are fulfilled when an appropriate mixture of two different molecular species (both bipolar or bipolar and monopolar) is used. According to the theory introduced by Israelachvili and co-workers, lipid self-assembly results from the balance of interaction free energy, entropy and molecular geometry. We have shown that this theory can be extended to bipolar lipids, in spite of their more complex nature, and the experimental results obtained combining ^{1}H-NMR, light scattering and entrapped volume techniques closely match theoretical expectations. To carry out calculations, it was necessary to introduce hypotheses about the disposition of bipolar molecules in the vesicle membrane. These hypotheses have been tested indirectly by measuring the transport properties mediated by carriers or channels, whose transport mechanism can be considered to be a probe of the membrane structure.

Introduction

The polar lipid extract (PLE) of the membrane of the thermophilic archaeobacterium *Sulfolobus solfataricus* is composed of several bipolar fractions, labeled P1, GL, SL and P2. Glycerol dialkyl glycerol tetraether (GDGT) and glycerol dialkyl nonitol tetraether (GDNT) constitute the backbone of all these fractions, which can be divided into two classes, the mono- and the bi-substituted molecules [1]. In the former (P1, GL, SL) a hydroxyl hydrogen is replaced by a polar group; in the latter (P2) hydroxyl hydrogens on both sides of the molecule are replaced by polar groups (see Fig. 1). It has been demonstrated that bisubstituted lipids from *Sulfolobus acidocaldarius* [2] can form liposomes in aqueous media. However, vesicles are not easily formed when large amounts of monosubstituted molecules are present, or when the hydrolitic fractions GDGT and GDNT are used [3,4]. Mixing egg phosphatidylcholine (egg PC) above a critical ratio with GDNT allows closed structures to be formed [3,4]. These vesicles are shown to be closed by ^{1}H-NMR spectra. In fact, the proton spectrum of choline-containing lipids exhibits resonances belonging to the headgroups and the hydrocarbon regions of the lipid molecules. The addition of paramagnetic ions to the external medium of the vesicles separates the interior and the exterior headgroup signal [5–7]. Thus, in binary mixtures, it is possible to monitor the formation of vesicles whose diameter has been deduced by light scattering or entrapped volume experiments. In the present work similar investigations have been carried out on several mixtures of monopolar with bipolar lipids. Moreover, it has been found that it is possible to obtain vesicles with pure bipolar lipids by increasing the amount of bisubstituted molecules (P2) in PLE.

In monopolar lipid systems the thermodynamic theory introduced by Israelachvili et al. [8] to predict the formation of vesicles and to prescribe their radius can be applied to pure lipids and to binary mixtures. However, in bipolar lipids, the fact that the chains have a double head imposes new constraints on the system. We have shown that in spite of the more complex nature of the molecules this theory still applies to bipolar lipids as well as monopolar-bipolar lipid systems and offers predictions that closely match the experimental results.

To apply the theory the molecular arrangement of bipolar lipids in the vesicles must be assigned. In fact, these molecules might assume three different configu-

Correspondence: A. Gliozzi, Dipartimento di Fisica, Università di Genova, 16146 Genova, Italy.

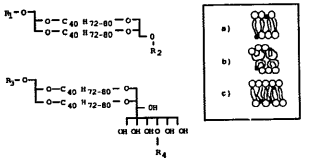

Fig. 1. Structure of isoprenoid ethers, backbone of complex lipids of thermophilic archaeobacteria. For GDGT $R_1 = R_2 = H$, for GDNT $R_3 = R_4 = H$. The polar lipid extract (PLE) is composed of P1 (7.8%); GL (19.5%); P2 (62.3%); SL (10.4%), where: P1 is a derivative of GDGT with R_1 = inositol-*P*, R_2 = H; GL is a mixture of: 70% derivative of GDNT with $R_3 = H$, $R_4 = \beta$-glcp and 30% derivative of GDGT with $R_1 = H$, $R_2 = \beta$-glcp-β-galp; P2 is a mixture of 90% derivative of GDNT with R_3 = inositol-*P* and $R_4 = \beta$-glcp, and 10% derivative of GDGT with R_1 = inositol-*P*, $R_2 = \beta$-glcp-β-galp; SL is a derivative of GDNT with: $R_3 = H$, $R_4 = \beta$-glcp-sulfate. The inset illustrates the different geometrical arrangements of molecules in a membrane. The small black circles indicate the unsubstituted glycerols ($R_1 = H$) while the big circles represent all other polar heads.

rations, as sketched in Fig. 1: fully extended, with the two polar heads on the two opposite surfaces of the membrane (a), assuming the shape of an arch (U-shaped configuration) (b) or the poorly hydrophilic polar head (the glycerol of Fig. 1) might partition in the apolar core (c). These different packing characteristics confer different transport properties to the vesicles. We have tested them using ionophores which are known to act as carriers or as channels in the membrane. In particular, it will be shown that transport mediated by a carrier formed by a single molecule is slightly sensitive to the packing characteristics of the lipid, while when the carrier is formed by self-assembly of several molecules, the packing characteristics become extremely important so that these molecules can be regarded as probes of the membrane structure.

Materials and Methods

Materials

Glycerol dialkyl glycerol tetraether (GDGT), glycerol dialkyl nonitol tetraether (GDNT), polar lipid extract (PLE) and the lipid fraction P2 were extracted from *Sulfolobus solfataricus* as described previously [9]. These lipids contain an average of 2.3 cyclopentane rings per chain, and can be assigned an average molecular weight of 1290, 1470, 1781 and 1872, respectively, for GDGT, GDNT, PLE and P2 (see Fig. 1). Egg PC was purchased from Lipid Products (Redhill, UK), praseodymium chloride ($PrCl_3 \cdot 6H_2O$) was obtained from Lancaster Synthesis (Lancaster, UK), deuterium oxide (^2H_2O, 99.8%) and the calcium ionophore A23187 were purchased from Aldrich Chemical Company (USA), sodium cholate and melittin (a channel former extracted from bee venom) were purchased from Sigma Chemical Company (USA), and the channel forming polypeptide alamethicin was a kind gift of Upjohn Company (Kalamazoo, MI, USA).

Preparation of lipid vesicles

Vesicles were prepared using sonication and dialysis [10]. In the first case, vesicles were prepared by pipetting the required amounts of egg PC and archaeobacterial lipids dissolved in organic solvents into a glass sonicating tube; GDNT, GDGT and egg PC were dissolved in chloroform, while PLE and P2 were dissolved in a mixture of chloroform/methanol/deuterium oxide (65:25:4, v/v/v). The solvents were evaporated under a stream of nitrogen and the last traces were removed by evacuating at 1 mmHg for 30 min. Since archaeobacterial lipids have a tendency to stick to the surfaces of the vessel, the sonicating tube was filled with nitrogen, sealed and shaken vigorously for a few hours to obtain a homogeneous liposomal preparation. A low power sonicating bath was sometimes required to free the lipid from the vessel surface. Unilamellar vesicles were obtained by sonication of the liposomes for 15 min at 60°C using a probe-type sonicator (Ultrasonic Ltd., UK), while passing a stream of nitrogen. Sonication was interrupted for 10–20 s every 2–3 min to avoid overheating. The vesicles were kept in a constant temperature controlled water bath at 60°C for 30 min to complete annealing. The second technique, which involves a standard procedure using the surfactant sodium cholate, was performed with the dialysis apparatus (Liposomat Dianorm, München). The ratio of lipid to detergent was 1:2 and the concentration of lipid in distilled water was 3 mg/ml. The dialysis was continued for 10–12 h. The latter vesicles were utilized only for light scattering measurements and not for transport studies since small residual traces of sodium cholate could act as an ionophore.

Light scattering

The diameter of the vesicles was measured through dynamic light scattering using a laser beam at 488 nm connected to a 60-channel Malvern correlator. Vesicle diameters above room temperature were measured using a laser at 514 nm connected to a Brookhaven Instrument BI 2030 digital correlator. The sample tube contained one milliliter of vesicles solution (filtered using a 220 nm Millex-GV Millipore filter) and the sampling time was 15 min.

^{1}H-NMR

The vesicular solution (0.5 ml) was pipetted into a 5 mm diameter NMR tube. ^{1}H-NMR spectra were obtained in a Varian FT NMR spectrometer operating at 80 MHz, fitted with a calibrated temperature con-

troller. Typically between 50 and 80 transients were collected prior to Fourier transformation. In order to separate the signal originating from the inner and outer lipid head groups, a known volume of a stock solution of $PrCl_3$ in ^2H_2O was added to the extravesicular space to obtain the desired concentration of Pr^{3+} ions. The shift of the external choline signal is caused by pseudo-contact interactions of Pr^{3+} which exchanges rapidly between the ^2H_2O and the phosphate sites on the headgroups of the outer monolayer [7]. Transmembrane transport of Pr^{3+} ions, initiating by adding the various ionophores, caused a time-dependent downfield shift of the NMR signal originating from the inner lipid headgroups. For A23187 a known volume of chloroform stock solution was added to an empty NMR tube, the solvent was carefully removed under a stream of nitrogen and the tube was evacuated at low pressure (1 mmHg). The vesicular dispersion (0.5 ml) was then added and incubated for 30 min at 50°C to allow partitioning of the ionophore in the membrane. The other ionophores (melittin, alamethicin and sodium cholate) were dissolved in ^2H_2O, introduced in the vesicular dispersion in the NMR tube and then incubated at 50°C for 30 min.

Calculation of parameters for self-assembly

The theory of lipid self-assembly has been developed and discussed by Israelachvili and co-workers [8,11]. The equations used in this work are briefly summarized below.

The minimum free energy of a single molecule in a self-aggregated structure is $\mu_N^0 = 2\gamma a_0$ where γ is the interfacial energy and a_0 is the optimal area per molecule. An amphipathic molecule may be able to pack into a variety of structures in which the molecular area remains close to a_0. In this case, the entropy term of the free energy will favour structures with the smallest aggregation number N. In turn, packing constraints due to molecular shape will determine the possible structures so that the molecular area leads to the lowest possible μ_N^0, which implies the lowest N at the same time. The critical packing condition is given by:

$$P_c = \frac{v}{a_0 l_c} \tag{1}$$

where v is the hydrocarbon volume and l_c is the maximum hydrocarbon length of the molecule. Bilayer vesicles are formed when $0.5 \leqslant P_c \leqslant 1$. In a vesicle system containing two components A and B, the lower limiting value from the outer vesicle radius, R_c, is given by the relationship:

$$R_c = \frac{l_c\left[3 + \sqrt{3(4\bar{r}/\bar{a}l_c - 1)}\right]}{6[1 - \bar{r}/\bar{a}l_c]} \tag{2}$$

where

$$\bar{a} = X_o a_A + (1 - X_o) a_B \tag{3}$$

is the mean outer monolayer lipid surface area,

$$\bar{r} = X_o r_A + (1 - X_o) r_B \tag{4}$$

is the mean outer monolayer lipid hydrocarbon volume and

$$X_o = \frac{A_o}{A_o + B_o} \tag{5}$$

is the molar fraction of lipid A in the outer monolayer.

The theory indicates that vesicles radii have a Gaussian distribution around the mean value R_c with standard deviation

$$\sigma_R \geqslant \frac{R_c}{l_c}\sqrt{\frac{kT}{\pi 8\gamma}} \tag{6}$$

where k and T have their usual meanings.

Results and Discussion

We have tested the applicability of the above theory to bipolar and monopolar/bipolar lipid systems. Geometrical parameters for egg PC were obtained from data found in the literature [12].

For bipolar lipids, the lengths of the acyl chains have been obtained from X-ray diffraction data [13,14] while the cross-sectional areas per polar head have been estimated comparing X-ray diffraction experiments and surface pressure-area isotherms [15]. The hydrocarbon volumes have been chosen according to the scheme in Fig. 2a. All dimensional parameters are given in Table I.

For one-component systems the critical packing parameter P_c can be evaluated just from the geometric data v, a_o, l_c. On the contrary, when binary mixtures are considered, a knowledge of X_o (Eqn. 5) is also required in order to calculate $\bar{a}$ and $\bar{r}$. Moreover, in those cases in which the two components had a different chain length l_c, the mean value $\bar{l}_c$ was used. X_o was determined through ^{1}H-NMR experiments and/or using simplifying assumptions about the disposition of the two molecular components. These assumptions have been suggested by analogies with X-ray diffraction data, or other experimental evidences and have been tested indirectly by transport measurements. When possible the error on P_c has also been evaluated. In all the other cases the theoretical results must be considered as estimates which, however, are good enough to match the experimental data, when the calculated vesicle radius R_c is compared with the experimental radius r_v. The standard deviation of the radii distribution

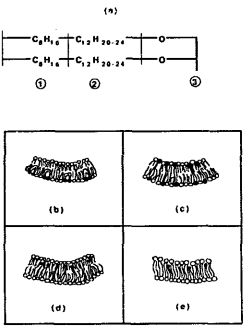

Fig. 2. (a) A bipolar lipid molecule can be divided into several parts in order to calculate the hydrocarbon volume: 1. the non-cyclic core; 2. the cyclopentane core; 3. the glycerol. (modified from Ref. 12). The proposed molecular arrangement of: GDGT/PC (b), P2/PC (c), GDNT/PC (d) and PLE/P2 (e).

(Eqn. 6) has been evaluated assuming $T = 300$ K and $\gamma \approx 50$ dyne/cm [11]. The results are given below and summarized in Table II, while detailed calculations can be found in the Appendix.

GDGT

When inserted in a membrane, a GDGT molecule can, in principle, adopt either a U-shaped or a straight configuration. In the former case the molecule would be bent, both polar ends being on the same side, while in the latter case the molecule spans the entire membrane thickness. In both configurations P_c is greater than one (1.13 ± 0.03). These results agree with our experimental finding that it is impossible to obtain closed structures only with GDGT molecules.

GDGT/egg PC mixtures were considered in order to investigate whether the addition of monopolar lipids might give rise to closed structures. We defined egg PC as component A and GDGT as component B. It has already been found from ^{1}H-NMR spectra that GDGT/egg PC in the molar ratio 1:4 do not form closed structures [3]. We found that closed vesicles were obtained when the PC content was increased to produce a 1:6 GDGT/PC molar ratio. In fact, it was possible to shift the signal of the outer monolayer choline headgroups of egg PC downfield, which indicates that vesicles are closed and are indeed impermeable to cations. The downfield peak remained unshifted for ten hours after adding Pr^{3+}. The ratio of the outer to the inner choline resonance A_o/A_i measured from NMR spectra was found to be 1. These results indicate that only a limited amount of GDGT can be accepted in closed vesicles, provided that the molecules bend and are mainly located on the outer monolayer (see Fig. 2b). Therefore, if we assume $B_i = 0$, we get $X_o = 0.75$. The critical packing parameter P_c is less than one (0.93) and the theoretical radius of vesicles R_c is 26 ± 3 nm, which agrees with $R_s = 25 \pm 4$ nm obtained by light scattering experiments.

TABLE I

Lipid molecular parameters

The parameters a_o, l_c, v are deduced from data in the literature [11–13]. For bipolar lipids l_c is half the value of the total length of the chains, while v has been calculated according to Fig. 2a. Volumes correspond to the average chemical composition.

Lipid	a_o (Å^2)	l_c (Å)	v (Å^3)
PC	71.7 ± 0.1	17.5 ± 0.1	1063 ± 1
GDGT	54 ± 1	16.5 ± 0.1	$2(V_1 + V_2) = 2017.6 \pm 0.4$
GDNT	60 ± 1	17.1 ± 0.6	$2(V_1 + V_2) + V_3 = 2106.6 \pm 0.5$
P1, GL, SL	80 ± 1	18.5 ± 0.1	$2(V_1 + V_2) + V_3 = 2106.6 \pm 0.5$
P2	80 ± 1	15.4 ± 0.1	$(V_1 + V_2) = 1008.8 \pm 0.2$

TABLE II

Critical packing parameter P_c and vesicle radius

The theoretical vesicle radius, R_c is compared with the experimental value R_s. When $P_c > 1$ no formation (n.f.) of vesicles occurs. For cases (a) and (b) of GDNT/PC see the text.

Lipid	P_c	R_c (nm)	R_s (nm)
GDGT	> 1	n.f.	n.f.
GDNT	> 1	n.f.	n.f.
PLE	> 1	n.f.	n.f.
GDGT/PC 1:6	0.93	26 ± 3	25 ± 4
GDNT/PC 1:4 (a)	0.90	22 ± 5	16.4 ± 0.3
GDNT/PC 1:4 (b)	0.92	21 ± 6	16.4 ± 0.3
GDNT/PC 1:8 (a)	0.87	15 ± 4	15.2 ± 0.3
GDNT/PC 1:8 (b)	0.89	15 ± 4	15.2 ± 0.3
PLE/P2 1:1	0.96	40 ± 4	45 ± 6
PLE/PC 1:4	–	–	57 ± 6

GDNT

Self-assembly of molecules in aqueous dispersions of this compound could occur in two different ways: with molecules in U-shaped or straight configurations. However, in both cases, the parameter P_c would be greater than one indicating that it is impossible to form vesicles with GDNT alone, as demonstrated also by experiments.

Mixing egg PC (component A) with GDNT (component B) above a critical ratio [3,4] allows vesicles to be formed. In this case, since there is no direct information about the disposition of GDNT molecules, X_o was calculated considering two limiting situations.

(a) GDNT molecules assume the configuration sketched in Fig. 2d. Nonitol heads are mainly located

in the outer layer due to curvature [4], while glycerols partition in the apolar core (as found, for instance, in the hexagonal phase of GDNT [13]). A GDNT/PC 1:4 molar ratio generates $X_o = 0.69$, $P_c = 0.90$ and $R_c = 22 \pm 5$ nm. A similar calculation for GDNT/PC 1:8 gives $X_o = 0.85$, $P_c = 0.89$ and $R_c = 15 \pm 4$ nm.

(b) GDNT molecules assume a U-shaped configuration and are located in the outer vesicle layer due to curvature. For GDNT/PC 1:4, $X_o = 0.69$, $P_c = 0.92$ and $R_c = 21 \pm 6$ nm. while for GDNT/PC 1:8, $X_o = 0.85$, $P_c = 0.87$ and $R_c = 15 \pm 4$ nm. In both cases the results obtained agree with the experimental radii of 16.4 ± 0.3 nm (GDNT/PC 1:4) and 15.2 ± 0.3 nm (GDNT/PC 1:8) measured by the entrapped volume technique [4]. This finding indicates that both configurations are consistent with thermodynamical and geometrical constraints, and might coexist together.

Complex lipids

PLE is a mixture composed of the lipid fractions P1, GL, SL and P2 (Fig. 1). P1, GL, SL (monosubstituted compounds, defined as component A) have an unsubstituted glycerol headgroup, while P2 (component B) has two polar heads. The geometrical parameters of these fractions are shown in Table I. The molar fraction X_o (Eqn. 5) has been calculated using the following assumptions. In a hypothetical PLE vesicle P2 molecules, endowed with big polar headgroups, should reasonably span the membrane. The number of polar heads is the same in the inner and outer layer, therefore we assume $B_o = B_i = B$. It is more likely that monosubstituted molecules should be oriented with their polar head on the outer side of the vesicle due to curvature, and their unsubstituted glycerols partition in the apolar core (as found by X-ray diffraction experiments in the lamellar phase of PLE [13]). Then we suppose $A_i \approx 0$. Knowing the molar ratio $A/B = 0.70 \pm 0.01$, we get $X_o = 0.41 \pm 0.01$ and $P_c = 1.11 \pm 0.06$. Therefore, closed vesicles are not supposed to form using PLE alone, a prediction which has been confirmed by our experiments.

On the other hand, closed vesicles were obtained by adding PC at a molar ratio PC/PLE 4:1 and 2:1. However, in these cases P_c cannot be calculated since the system is a three-component mixture and there is no information about the composition of the external layer and the arrangement of asymmetric molecules in the vesicle.

A mixture of PLE and P2 in the molar ratio 1:1 produces vesicles whose radius is $R_s = 45 \pm 6$ nm (light scattering results). Since there is no egg PC in this lipid mixture, we used electron microscopy techniques, instead of ^{1}H-NMR, to monitor vesicle formation [16]. The calculation of P_c in this case is analogous to the previous one for PLE; the only change is in the molar ratio monosubstituted molecules/P2, which now is 0.26. Therefore, $X_o = 0.21$, $P_c = 0.96$ and $R_c = 40 \pm 4$ nm, which agrees with the experimental value.

Ionophores as probes of membrane structure

It may be possible to obtain further information about membrane lipid organization from transport properties in the presence of ionophores.

The addition of the lanthanide Pr^{3+} to the external vesicular medium shifts the ^{1}H-NMR signal from the outer choline headgroup downfield [7]. In the absence of ionophores the signals from the inner and outer choline headgroups are unaffected up to several days, indicating that the vesicles remain impermeable to the probe ion Pr^{3+}. However, in the presence of an ionophore, a time-dependent downfield shift of the inner choline peak is observed and indicates that facilitated transport of the ion across the vesicle bilayer is taking place. The plot of the inner peak shift against time is linear before the outer and inner peak appreciably merge. Shifts in the inner signal can be converted into intravesicular Pr^{3+} concentrations using calibration graphs [17]. This procedure is not needed in the present case. In fact, we are interested in the comparison of the transport properties through mixed and pure PC vesicles. The rate of transport with reference to PC can be simply derived from the ratios of the slopes of the time-dependent shifts in the linear region. These ratios are collected in Table III and summarize the transport results which will be analyzed in the discussion below.

A23187 is an antibiotic containing a carboxylic group $C_{29}H_{37}N_3O_6$ (Fig. 3b). This molecule binds bi-trivalent ions and transports them across the bilayer [18]. It has been shown that Pr^{3+} ions are carried in the membrane by a single ionophore molecule as a 1:1 complex. Pr^{3+} transport across vesicles made of P2/PC

TABLE III

Ionophore mediated vesicle permeability to Pr^{3+}

P/P_o is the permeability ratio with respect to PC. The molar ratio (m.r.) of the lipid mixtures is indicated.

Ionophore	Lipid mixture	m.r.	T	P/P_o
A23187	GDGT/PC	1:6	60°C	~0
(carrier)	GDNT/PC	1:4	60°C	0.2
	P2/PC	1:2	60°C	0.2
	P2/PC	1:4	60°C	0.8
	PLE/PC	1:4	40°C	0.6
	PLE/PC	1:4	50°C	0.7
	PLC/PC	1:4	60°C	1
Na cholate	GDGT/PC	1:6	60°C	~0
(carrier)	GDNT/PC	1:4	60°C	~0
	PLE/PC	1:4	60°C	~0
	P2/PC	1:2	40°C	0.2
Alamethicin (channel forming)	PLE/PC	1:4	60°C	0.7

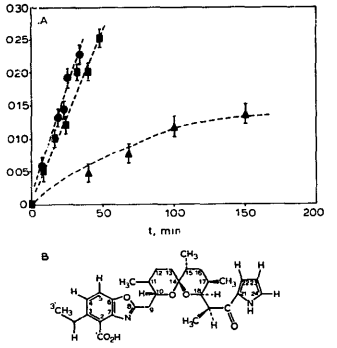

Fig. 3. (A) The downfield shift, δ, of the inner choline resonance representing A23187-mediated Pr^{3+} transport in P2/PC 1:4 (■) and 1:2 (▲) molar ratio compared with pure PC (●) vesicles. $T = 60°C$. In all figures the dashed line has been drawn only to make it easier to read the graph. (B) The chemical structure of A23187.

(1:4 and 1:2 molar ratio) and pure PC have been investigated in the presence of this carrier at a lipid/carrier molar ratio of 1300:1 and at 5 mM Pr^{3+}. The data are shown in Fig. 3. The downfield shift, δ, of the inner choline resonance is plotted as a function of time immediately after the addition of Pr^{3+}. It can be observed that the rate of transport is higher in pure PC vesicles, while it decreases by increasing the bipolar lipid concentration. The deviation from linearity indicates that the system is reaching equilibrium. Fig. 4 shows the transport induced in PLE/PC vesicles (1:4 molar ratio) and in pure PC by the same ionophore concentration. The experiments have been performed at three different temperatures ranging from 40 to 60°C. It is interesting to observe that at 40°C there is a great difference in permeability of the two kinds of vesicles, while when increasing the temperature to 60°C, an almost identical kinetic behaviour is observed. Fig. 4 also shows the permeability induced by this carrier in GDNT/PC vesicles (molar ratio 1:4) at 60°C. By contrast no transport was induced in GDGT/PC vesicles (1:6 molar ratio). This behaviour indicates that an increase in the complexity of the lipid disposition, decreases the rate of transport mediated by this ionophore. For GDNT/PC vesicles the theory could not discriminate between the configuration (a), shown in Fig. 2d, and the U-shaped configuration (b). Comparing the transport results of GDNT/PC with those of GDGT/PC, in which the U-shaped configuration completely inhibits Pr^{3+} transport, the (b) configuration appears rather unlikely.

It is well known that the bile salt sodium cholate highly increases membrane permeability [19]. An aggregate of four molecules forms an inverted micelle which is incorporated in the lipid bilayer forming a hydrophilic cavity for ions. In our experiments the molar ratio of lipid to carrier was constant in all preparations and equal to 12, while the number of Pr^{3+} ions per choline polar group was 0.1. In contrast with the results obtained with the ionophore A23187, sodium cholate does not induce any Pr^{3+} ion transport at 60°C in PLE/PC (1:4) vesicles. The same result has been obtained with GDGT/PC (1:6) and GDNT/PC (1:4). However, this bile salt has shown some Pr^{3+} transport in P2/PC vesicles (molar ratio 1:2) although at a lower rate compared with pure PC vesicles (Fig. 5). This behaviour may be due to the lower complexity of P2/PC lipid system. In fact, the molecular arrangement in these vesicles (Fig. 2c) is very similar to the usual bilayer structure.

The channel-forming ionophores melittin [20] and alamethicin [21] were also employed to check transport properties. Melittin, a polypeptide with 26 amino acids, is the main component of bee venom. Its mechanism of action as an ionophore is not very well known. Studies on planar lipid bilayers [22] have shown that melittin, added to the aqueous phase, binds strongly to the interface, dipping into the lipid core without actually spanning it. This interaction lowers the energy barrier for permeation of hydrophilic ions. Pr^{3+} transport induced by this ionophore in egg lecithin vesicles at a concentration of 600 μg per 1 ml of egg PC vesicles (20 μg/ml), is shown in Fig. 6, while no Pr^{3+} ion transport has been observed in PLE/PC (1:4) vesicles. This

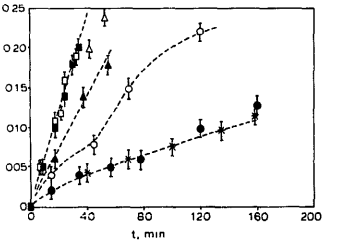

Fig. 4. The downfield shift, δ, of the inner choline resonance representing A23187-mediated Pr^{3+} transport at different temperatures in vesicles of PC (empty points) and PLE/PC 1:4 molar ratio (filled points). (○, ●) 40°C, (△, ▲) 50°C, (□, ■) 60°C. (•) GDNT/PC 1:4 molar ratio at 60°C.

indicates the lack of any facilitated permeability pattern in the more complex PLE/PC system.

In the case of alamethicin it is well known that channels are formed by several monomers spanning the entire membrane thickness [23]. Experiments on the conductivity of planar lipid membranes indicate that the higher-conducting alamethicin channels are formed by an increase in the average diameter which is determined by the number of monomers forming the channel. Studies on DPPC vesicles [24] have indicated the formation of narrow channels, with four ionophore molecules per channel. A slow rate of Pr^{3+} transport was induced by alamethicin in PLE/PC (1:4) vesicles. Fig. 6 shows this result, together with that obtained in pure PC vesicles. Since this ionophore spans the entire membrane thickness, transport properties are less sensitive to the packing characteristics of the lipids. Nevertheless, Fig. 6 shows that in PLE/PC the transport occurs at a lower rate, compared to PC vesicles. This fact could be related to the negative charge carried on the lipid by the phosphomyoinositol groups and on the polypeptide by glutamic acid.

Conclusions

We have shown that the Israelachvili model [8] can be applied to water dispersions of bipolar and monopolar lipid mixtures. Electron microscopy has shown that lipid dispersions exhibit complex morphologies when $P_c > 1$ [3,16]. When $P_c < 1$ vesicles are formed and the agreement between the theoretical and experimental results in predicting their average diameter is rather

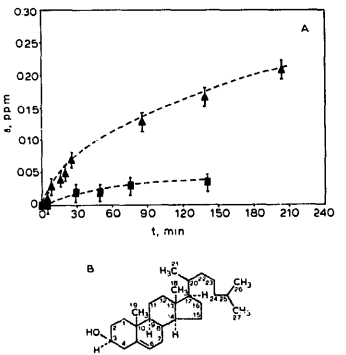

Fig. 5. (A) The downfield shift, δ, of the inner choline resonance representing Na cholate mediated Pr^{3+} transport. Vesicles of: PC (▲), and 1:2 molar ratio P2/PC (■). $T = 40°C$, Na cholate 2 mM, Pr^{3+} 5 mM. (B) The chemical structure of the sodium cholate.

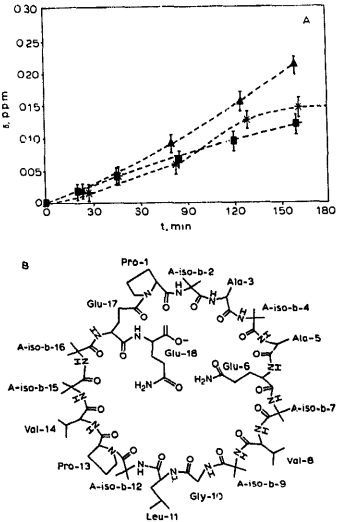

Fig. 6. (A) The downfield shift, δ, of the inner choline resonance representing alamethicin-mediated Pr^{3+} transport across vesicles of: (▲) PC, and 1:4 molar ratio PLE/PC (■). Lipid/polypeptide molar ratio 600:1, and Pr^{3+} concentration 5 mM. $T = 60°C$. The transport mediated by melittin in PC vesicles (•) at 60°C is also shown. (B) The chemical structure of alamethicin.

good, as shown in Table II. Moreover, since bipolar lipids can assume several configurations, as indicated in Figs. 1 and 2, it is generally possible to assign a precise configuration to the molecules.

Further information on the packing characteristics of the lipid molecules is obtained by the rate of transport of Pr^{3+}, mediated by carriers or channels. The results are summarized in Table III and indicate that the ionophores can be considered as probes of the membrane structure. In fact, it has been shown that whenever a single molecule is involved in facilitated transport, like in the case of A23187, a very important factor affecting the transport rate is the fluidity of the apolar chains. As a consequence, the Pr^{3+} transport rate increases by increasing the PC content or increasing the temperature, and at 60°C it may reach the value of egg PC (this is the case for PLE/PC and P2/PC) (1:4 molar ratio). However, the fluidity of the system is not the only parameter affecting transport. In fact, although ESR experiments on GDNT have shown

that the mobility of the chains at $T \geq 60°C$ is similar to that of egg PC in normal physiological conditions [25], the rate of transport shown in Fig. 4 in GDNT/PC is much smaller than in pure PC or in PLE/PC vesicles. This probably occurs as the result of the more complex configuration of the glycerols head groups (partitioning in the apolar core as shown in Fig. 2d), which are present at a much higher percentage in GDNT/PC with respect to PLE/PC vesicles. Finally, when the structure of the lipid vesicle is extremely complex (as in the case of GDGT/PC of Fig. 2b), even a simple carrier molecule like A23187 is unable to induce transport.

When the transport involves the aggregation of several molecules more severe restrictions on transport are observed. In this case, only when the bipolar lipids assume a straight configuration, as in the case of P2/PC, the rate of Pr^{3+} transport does not considerably differ from the one observed in a characteristic monopolar lipid vesicle, like egg PC. In all the other cases, when part of the lipid molecules are in a complex configuration, the transport is completely inhibited or extremely low (this is the case for GDGT/PC, GDNT/PC, PLE/PC with Na-cholate or PLE/PC with melittin). Only alamethicin, a channel spanning the entire thickness of the membrane, does not drastically change its transport properties. This result is very interesting because it indicates that, provided the channel is formed and in contrast to a carrier system, only minor modulations in transport are caused by the lipid environment.

Appendix

GDGT

In the U-shaped configuration, $v = 2(V_2 + V_1)$ and $a_0 = 108$ Å^2 (the area occupied by two polar heads). Taking l_c as in Table I, P_c turns out to be greater than one (1.13 ± 0.03). Since the molecule is supposed to span the entire membrane thickness in the straight configuration, the calculation of the packing parameter must be performed considering just half of the molecule ($v = V_1 + V_2$, a_0 and l_c as in Table I). Therefore, also in this case, $P_c = 1.13 \pm 0.03$.

GDGT/PC 1:6

^{1}H-NMR spectra of vesicles composed of GDGT/PC 1:6 gave a ratio of the outer to the inner choline resonance A_o/A_i equal to one. By simple geometrical arguments this means that GDGT molecules are mainly located in the outer vesicle layer; such a disposition is possible if molecules assume a U-shaped configuration. Therefore, assuming $B_i = 0$ and observing that $(A_o + A_i)/B_o = 6$, we get $X_o = A_o/(A_o + B_o) = 6/(7 + (A_i/A_o)) = 0.75$. Then, using data in Table I, we obtain $\bar{a} = 80.8$ Å^2, $\bar{v} = 1301.7$ Å^3, $\bar{l}_c = 17.3$ Å, and finally $P_c = 0.93$ and $R_c = 26 \pm 3$ nm.

GDNT

In the straight configuration the molecule is supposed to span the entire membrane thickness. Therefore only half of the molecule has to be considered, and a hypothetical GDNT vesicle can be treated as a binary mixture of molecules having either nonitol (component A) or glycerol (component B) as polar heads. The critical packing parameter P_c was calculated for several values of X_{o_2} using $v = V_1 + V_2 = 1008.8 \pm 0.2$ Å^3, $l_c = 17.1 \pm 0.6$ Å, a_A and a_B, respectively, the nonitol and glycerol areas (the former assumed to be equal to the area of GDNT, and the latter equal to the area of GDGT in Table I). We found that for $0.5 \leq X_o \leq 0.9$ P_c is in the range from 1.03 ± 0.05 to 0.99 ± 0.05. Therefore, the higher the asymmetry, the lower the value of P_c although it is approximately equal to one. This fact indicates that it is possible to form planar bilayers using this compound, as it was found previously [26]. It is worth noting that the U-shaped configuration corresponds exactly to the case $X_o = 0.5$ in the straight configuration.

GDNT/PC 1:4

^{1}H-NMR spectra of vesicles composed of GDNT/PC 1:4 gave a ratio of the outer to the inner choline resonance $A_o/A_i = 1.3$. In order to calculate X_o, two different dispositions of GDNT molecules were considered as limiting situations.

(a) GDNT molecules are in the configuration sketched in Fig. 2d, the nonitol heads being located in the outer layer and the glycerols partitioning in the apolar core, which means $B_i = 0$ and $B_o = B$. Observing that $(A_o + A_i)/B = 4$, one gets $X_o = 4/((5 + (A_i/A_o)) = 0.69$. Then, assuming that l_c for GDNT molecules in the straight configuration is equal to 34.1 Å [13], and taking other geometrical parameters as in Table I, we have $\bar{a} = 68.1$ Å^2, $\bar{v} = 1386.5$ Å^3 and $\bar{l}_c = 22.6$ Å. Therefore, $P_c = 0.90$ and $R_c = 22 \pm 5$ nm.

(b) GDNT molecules are in a U-shaped configuration and are located in the outer layer. The results for X_o is therefore the same as in (a). But now the geometrical parameters for GDNT are: $a = 114$ Å^2 (the sum of the nonitol and glycerol areas) $v = 2017.6$ Å^3 (since the glycerol is assumed to be in the polar moiety) and $l_c = 17.1$ Å. Since the parameters for egg PC are unchanged, $\bar{a} = 84.8$ Å^2, $\bar{v} = 1358.9$ Å^3, $\bar{l}_c = 17.4$ Å and finally $P_c = 0.92$ and $R_c = 21 \pm 6$ nm.

GDNT/PC 1:8

In this case, the ratio A_o/A_i obtained from ^{1}H-NMR measurements is equal to 1.6. The calculations were carried out using the same assumptions as in the case of GDNT/PC 1:4. The results obtained in the straight configuration (a) are $X_o = 0.85$, $P_c = 0.87$, $R_c = 15 \pm 4$ nm, and in the U-shaped configuration (b) $X_o = 0.85$, $P_c = 0.89$, $R_c = 15 \pm 4$ nm.

PLE

The weight composition of PLE is (62.3 ± 0.3)% P2 and (37.7 ± 0.5)% monosubstituted compounds, which means, (assuming that the molecular weights of P2 and the monosubstituted fractions are, respectively, 1872 and 1629), $(A_0 + A_1)/B = 0.70 \pm 0.01$. Since P2 molecules are supposed to extend through the membrane, the number of P2 polar heads is the same in the inner and the outer layer. Therefore, $B_i = B_o = B$. To calculate P_c we further assume $A_i = 0$, which means that the polar headgroups of monosubstituted molecules are found on the outer side only, while the unsubstituted glycerols partition in the apolar core. With these hypotheses, $X_o = A_o/(A_o + B_o) = 0.41 \pm 0.01$. Using data in Table I we get $\bar{a} = 80 \pm 1$ Å^2, $\bar{v} = 1460 \pm 30$ Å^3, $\bar{l}_c = 16.4 \pm 0.4$ Å and finally $P_c = 1.11 \pm 0.06$.

PLE / P2 1:1

In a mixture PLE/P2 1:1 the molar ratio between monosubstituted molecules (component A) and P2 (component B) is $(A_o + A_i)/B = 0.26$. With the same assumptions used above ($A_i = 0$ and $B_o = B$) we get $X_o = A_o/(A_o + B) = 0.21$. From data in Table I we have $\bar{a} = 80$ Å^2, $\bar{v} = 1240$ Å^3, $\bar{l}_c = 16.1$ Å, which give $P_c = 0.96$ and $R_c = 40 \pm 4$ nm.

Acknowledgements

We thank Dr. R. Rolandi for many stimulating discussions and Dr. A. Sanguineti for help with light scattering measurements. The technical help of R. Di Maso and E. Pagnotta is also greatly acknowledged. This work has been supported by the Italian Ministery of University and Scientific Research (MURST) 60% and 40% grants, by CNR grant 'Progetto Finalizzato Chimica Fine II' and by CEE Esprit Basic Research Action N. 3200.

References

1 De Rosa, M., Gambacorta, A. and Gliozzi, A. (1986) Microbiol. Rev. 50, 7–80.
2 Lo, S.L. and Chang, E.L. (1990) Biochem. Biophys. Res. Commun. 167, 238–243.
3 Mirghani, Z., Bertoia, D., Gliozzi, A., De Rosa, M. and Gambacorta, A. (1990) Chem. Phys. Lipids 55, 85–96.
4 Lelkes, P.I., Goldenberg, D., Gliozzi, A., De Rosa, M., Gambacorta, A. and Miller, I.R. (1983) Biochim. Biophys. Acta 732, 714–718.
5 Bystrov, V.F., Dubrovina, N.I., Barsukov, L.I. and Bergelson, L.D. (1971) Chem. Phys. Lipids 6, 343–350.
6 Fernandez, M.S., Celis, H. and Montal, M. (1973) Biochim. Biophys. Acta 323, 600–605.
7 Barsukov, L.I., Viktorov, A.V., Vasilenko, I.A., Erastingueera, R.P. and Bergelson, L.D. (1980) Biochim. Biophys. Acta 598, 158–168.
8 Israelachvili, J.N., Marcelja, S. and Horn, R.G. (1980) Q. Rev. Biophys. 13, 121–200.
9 De Rosa, M., Gambacorta, A., Nicolaus, B., Chappe, B. and Albrecht, P. (1983) Biochim. Biophys. Acta 753, 249–256.
10 Weder, H.G. and Zumbuehl, O. (1988) in Liposome Technology, Vol. 1, pp. 80–105, CRC Press, Boca Raton.
11 Israelachvili, J.N., Mitchel, D.J. and Ninham, B.W. (1977) Biochim. Biophys. Acta 470, 185–201.
12 Carnie, S., Israelachvili, J.N. and Painthorpe, E.A. (1979) Biochim. Biophys. Acta 554, 340–357.
13 Gulik, A., Luzzati, V., De Rosa, M. and Gambacorta, A. (1985) J. Mol. Biol. 182, 131–149.
14 Gulik, A., Luzzati, V., De Rosa, M. and Gambacorta, A. (1988) J. Mol. Biol. 201, 429–435.
15 Rolandi, R., Schindler, H., De Rosa, M. and Gambacorta, A. (1986) Eur. Biophys. J. 14, 19–27.
16 Relini, A., Cavagnetto, F. and Gliozzi, A. (1992) in Proceedings of the International Workshop on Amphiphilic Membranes (Lipowsky, R., ed.), Springer, Heidelberg, in press.
17 Hunt, G.R.A., Tipping, L.R.H. and Belmont, M.R. (1978) Biophys. Chem. 8, 341–355.
18 Hunt, G.R.A. (1975) FEBS Lett. 58, 194–196.
19 Hunt, G.R.A. and Jawaharlal, A. (1980) Biochim. Biophys. Acta 601, 678–684.
20 Hunt, G.R.A., Jones, I.C. and Veiro, J.A. (1984) Biosci. Rep., 4, 403–413.
21 Haydon, D.A. and Hladky, S.B. (1972) Q. Rev. Biophys. 5, 187–282.
22 Schoch, P. and Sargent, D.F. (1980) Biochim. Biophys. Acta 602, 234–247.
23 Eisenberg, M., Kleinberg, M.E. and Shaper, J.H. (1977) Ann. N.Y. Acad. Sci. 303, 281–291.
24 Hunt, G.R.A. and Jones, I.C. 91982) Biosci. Rep. 2, 921–928.
25 Bruno, S., Cannistraro, S., Gliozzi, A., De Rosa, M. and Gambacorta, A. 91985) eur. Biophys. J. 13, 67–76.
26 Gliozzi, A., Rolandi, R., De Rosa, M. and Gambacorta, A. (1982) Biophys. J. 37, 563–566.